

2019

# Differentiating between the tumor microenvironment and inflammation in order to use immune cells as living cell diagnostics for early cancer detection

---

<https://hdl.handle.net/2144/36247>

*Downloaded from DSpace Repository, DSpace Institution's institutional repository*

BOSTON UNIVERSITY  
SCHOOL OF MEDICINE

Thesis

**DIFFERENTIATING BETWEEN THE TUMOR MICROENVIRONMENT AND  
INFLAMMATION IN ORDER TO USE IMMUNE CELLS AS LIVING CELL  
DIAGNOSTICS FOR EARLY CANCER DETECTION**

by

**SANDHYA BODAPATI**

B.S., Santa Clara University, 2017

Submitted in partial fulfillment of the  
requirements for the degree of  
Master of Science

2019

© 2019 by  
SANDHYA BODAPATI  
All rights reserved

Approved by

First Reader

---

Louis C. Gerstenfeld, Ph.D.  
Professor of Orthopaedic Surgery

Second Reader

---

Sanjiv S. Gambhir, MD, Ph.D.  
Professor of Radiology

## **ACKNOWLEDGMENTS**

I would like to acknowledge my research mentors, Dr. Gayatri Gowrishankar and Dr. Ataya Sathirachanda for their guidance and constant help throughout this research project. Thank you for helping me grow as a researcher, and for teaching me many laboratory techniques. I would also like to acknowledge Dr. Sanjiv Sam Gambhir for the opportunity to conduct research in his laboratory, and for his insight in helping plan this research project. Finally, I would like to acknowledge Dr. Louis Gerstenfeld and my professors at Boston University School of Medicine for helping fuel my passion for science and medicine.

**DIFFERENTIATING BETWEEN THE TUMOR MICROENVIRONMENT AND  
INFLAMMATION IN ORDER TO USE IMMUNE CELLS AS LIVING CELL  
DIAGNOSTICS FOR EARLY CANCER DETECTION**

**SANDHYA BODAPATI**

**ABSTRACT**

Recent advances in the field of synthetic biology have enabled the use of macrophages as living cell diagnostics for early cancer detection. Presently, macrophages have been engineered to be macrophage sensors, which produce a reporter signal upon activation of the ARG1 promoter—an event which will occur in the tumor microenvironment (Aalipour et al., 2019). Incorporation of Boolean logic gates can help refine the specificity of this sensor, to ensure that it is only activated in the tumor microenvironment and not in inflammatory or wound healing environments. In order to do this, it is necessary to identify genes that can be used as markers that are differentially specific to tumor microenvironments compared to inflammatory microenvironments. Because tumor microenvironments are commonly infiltrated with M2-polarized macrophages and inflammatory environments are commonly infiltrated with M1-polarized macrophages, assessing relative gene expression from M1 and M2 type macrophages could be a useful avenue for identifying genes to be used in Boolean logic gates for enhancing the specificity of the previously developed macrophage sensor. First, macrophages must be polarized to the M1 and M2 phenotypes, and second, quantitative real time PCR must be used to identify genes that are upregulated in either M1s or M2s.

## TABLE OF CONTENTS

TITLE.....	i
COPYRIGHT PAGE.....	ii
READER APPROVAL PAGE.....	iii
ACKNOWLEDGMENTS .....	iv
ABSTRACT.....	v
TABLE OF CONTENTS.....	vi
LIST OF TABLES.....	ix
LIST OF FIGURES .....	xi
LIST OF ABBREVIATIONS.....	xiii
INTRODUCTION .....	1
<b>The Need for Early Cancer Detection.....</b>	<b>1</b>
<b>Applications of Synthetic Biology for Early Diagnosis.....</b>	<b>2</b>
<b>Boolean Logic Gates .....</b>	<b>4</b>
<b>Luciferase Reporters .....</b>	<b>5</b>
<b>Immunology and Cancer.....</b>	<b>6</b>
<b>A Novel Field: Use of Immune Cells for Cancer Detection.....</b>	<b>8</b>
<b>Macrophage Biology.....</b>	<b>8</b>
<b>Arginase 1 .....</b>	<b>11</b>

<b>Proof of Concept Macrophage Sensor .....</b>	<b>12</b>
<b>Improvements for the Macrophage Sensor .....</b>	<b>14</b>
<b>Specific Aims .....</b>	<b>14</b>
<b>METHODS .....</b>	<b>15</b>
<b>Macrophage Cell Lines.....</b>	<b>16</b>
<b>RNA Expression Analysis .....</b>	<b>21</b>
<b>ELISA Cytokine Analysis .....</b>	<b>23</b>
<b>Identifying Gene Candidates for "AND" and "NOT" Gates.....</b>	<b>23</b>
<b>RESULTS .....</b>	<b>25</b>
<b>Murine Macrophage Polarization .....</b>	<b>25</b>
<b>Human Macrophage Polarization .....</b>	<b>25</b>
<b>Identification of "AND" and "NOT" Gates.....</b>	<b>29</b>
<b>Testing Gene Candidates from the iPRECOG Database.....</b>	<b>30</b>
<b>DISCUSSION.....</b>	<b>32</b>
<b>RAW264.7 Cell Line .....</b>	<b>32</b>
<b>Macrophage Polarization Methods for RAW264.7 .....</b>	<b>33</b>
<b>Human Monocyte Cell Lines.....</b>	<b>36</b>
<b>Macrophage Polarization Methods for THP-1.....</b>	<b>37</b>
<b>"AND" and "NOT" Gate Gene Candidates from the iPRECOG Database.....</b>	<b>38</b>
<b>Limitations.....</b>	<b>39</b>
<b>Next Steps .....</b>	<b>40</b>
<b>Clinical Translation .....</b>	<b>41</b>



REFERENCES .....	43
VITA.....	47

## LIST OF TABLES

Table	Title	Page
1	Relative ARG1 expression in RAW264.7 cells that have been activated to become polarized macrophages with different treatment conditions.	23
2	Relative iNOS expression in RAW264.7 cells that have been activated to become polarized macrophages with different treatment conditions.	23
3	Relative IL-10, an M2 marker, expression in THP-1 cells that have been activated to become polarized macrophages with different treatment conditions.	26
4	Genes upregulated in M2s and expressed at low levels in M1s, identified using iPRECOG data (Stanford University, 2019).	27
5	Genes upregulated in M1s and expressed at low levels in M2s, identified using iPRECOG data (Stanford University, 2019).	27
6	Relative DPEP2 expression levels in polarized macrophages prepared from the THP-1 cell line.	28

7	Relative HRH1 expression levels in polarized macrophages prepared from the THP-1 cell line.	28
8	Relative SPIB expression levels in polarized macrophages prepared from the THP-1 cell line.	29

## LIST OF FIGURES

Figure	Title	Page
1	Applying a mathematical model to measure the growth of an asymptomatic tumor.	2
2	Schematic depicting the use of Boolean logic gates to improve the specificity of an engineered cell circuit.	4
3	A few macrophage polarization outcomes and their transcriptional profiles.	10
4	Schematic for use of macrophages as living cell diagnostics.	12
5	RAW264.7 cells viewed with a 400x optical microscope.	15
6	THP-1 cells viewed with a 200x optical microscope under different treatment conditions.	19
7	CXCL11 expression is strongest in THP-1 cells treated with LPS and IFN $\gamma$ , or M1 polarized macrophages.	24
8	ELISA result for TNF $\alpha$ expression in THP-1 cells that have been activated to become macrophages with different treatment conditions.	25

9	ELISA result for IL-10 expression in THP-1 cells that have been activated to become macrophages with different treatment conditions.	26
10	Relative ARG1 expression in RAW264.7 cells treated with IL-4 alone and IL-13 alone compared to untreated cells.	32

## LIST OF ABBREVIATIONS

APC.....	Antigen Presenting Cell
ARG1.....	Arginase 1
ATCC.....	American Type Culture Collection
CAR.....	Chimeric Antigen Receptor
CARMA.....	Chimeric Antigen Receptor Macrophages
C <sub>q</sub> .....	Quantification Cycle
CSF-1R.....	Colony Stimulating Factor-1 Receptor
CXCL11.....	C-X-C Motif Chemokine Ligand 11
DMEM.....	Dulbecco's Modified Eagle Media
DPEP2.....	Dipeptidase2
FBS.....	Fetal Bovine Serum
GAPDH.....	Glyceraldehyde 3-phosphate Dehydrogenase
GEM.....	Genetically Engineering Macrophage
Gluc.....	<i>Gaussia</i> luciferase
IFN $\gamma$ .....	Interferon $\gamma$
IL.....	Interleukin
iNOS.....	Inducible Nitric Oxide Synthase
M1.....	Classically Activated Macrophage
M2.....	Alternatively Activated Macrophage
PLAP.....	Placental Alkaline Phosphatase
PMA.....	Phorbol Myristate Acetate

qPCR.....	Quantitative Polymerase Chain Reaction
RPMI.....	Roswell Park Memorial Institute Media
RT-PCR.....	Reverse Transcription Polymerase Chain Reaction
SEAP.....	Secreted Embryonic Alkaline Phosphatase
SPIB.....	SPi-B Transcription Factor
TAM.....	Tumor Associated Macrophage
UV.....	UltraViolet
VEGF.....	Vascular Endothelial Growth Factor

## INTRODUCTION

Cancer is a leading cause of death around the world, despite numerous advances in this field of medicine in the past century (Shamsi & Islamian, 2010). Early detection of cancer cells would revolutionize the way cancer is treated, and save millions of lives and resources invested into healthcare. While early detection may sound like a simple task, early identification of cancer cells is challenging for various reasons. There is typically a gap of years between the inception of the first neoplastic cells in one's body and the time that they are detectable by clinical imaging. (Shamsi & Islamian, 2010). In fact, mathematical models have calculated this period of preliminary growth before tumor cells can be imaged clinically (Hori, Lutz, Paulmurugan & Gambhir, 2017). Tumors must be at a size of 6.24 mm to be detected with clinical imaging, and this size is reached approximately 50 months following the birth of asymptomatic tumor cells (Hori, Lutz, Paulmurugan & Gambhir, 2017). This model is shown in **Figure 1**.

### *The Need for Early Cancer Detection*

More often than not, in clinics today, cancer is identified in stages III and IV, and by this point, though doctors try to limit the spread of metastases, success rates are low (Shamsi & Islamian, 2010). The earlier cancer is detected, the more likely there is a chance of a positive treatment outcome. The medical community still lacks the technology to detect the first few divisions of neoplastic cells in a noninvasive manner, before they metastasize throughout the body (International Atomic Energy Agency, 2010). Blood tests are widely used clinically to assess the levels of cancer biomarkers



from tumors and the severity of cancer, but this does not address preventative care; further research is needed to apply this principle to preventative stages, in order to identify the conception of the first tumor cells in one's body (Shamsi & Islamian, 2010).

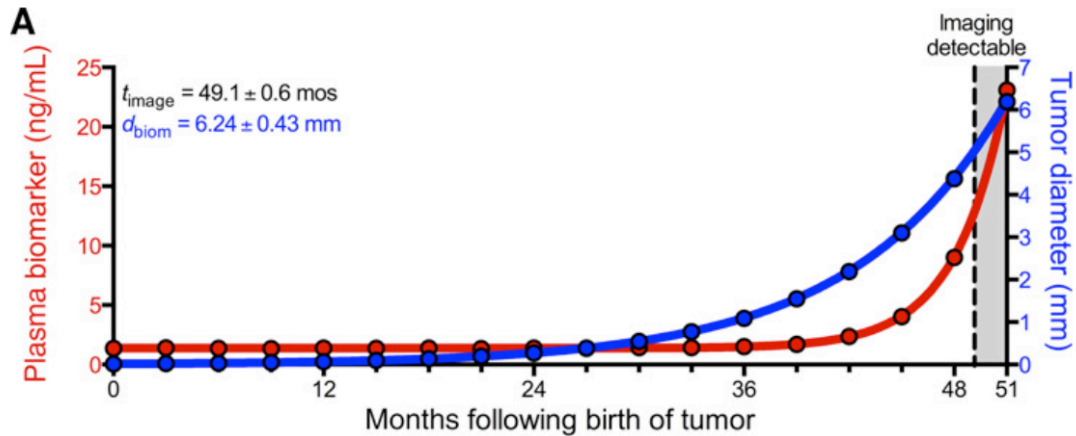


**Figure 1. Applying a mathematical model to measure the growth of an asymptomatic tumor.** Plasma biomarker levels were measured using blood tests every 3 months until the tumor was detectable with imaging. While  $t_{\text{image}}$  reflects imaging detectability,  $d_{\text{biom}}$  reflects estimated tumor diameter based on the plasma biomarker level. Figure taken from (Hori, Lutz, Paulmurugan & Gambhir, 2017).

### *Applications of Synthetic Biology for Early Diagnosis*

The field of synthetic biology paves way for the use of living cell diagnostic techniques for early cancer detection (Sedlmayer, Aubel, & Fusseneger, 2018). Synthetic biology refers to the use of genetic engineering principles to modify existing circuitry in cells and microorganisms to produce a desired function or response. Synthetic biology has huge applications in the field of early disease detection. For example, a sensor that monitors levels of histamine release in the body by producing a reporter protein upon histamine detection has allowed for sensitive and easy monitoring of allergens and

allergic disorders in sensitive patients (Auslander et al., 2014). Modification of microorganisms such as *Salmonella typhi* by manipulation of quorum-sensing and autoinduction has been applied to early cancer detection and even treatment via antitumor drug release (Din et al., 2016). The use of synthetic biology to engineer living cells and other sensors for early detection of disease demonstrates key advantages to traditional blood-based biomarker analysis due to the sensitivity of genetic approaches to disease detection. Living cell diagnostics can detect disease at its conception, thereby serving as a method for monitoring a patient's health. Furthermore, living cell diagnostics can identify disease even before it is detectable through clinical blood tests, which leads to better patient prognosis.

However, in the context of cancer, several challenges remain with regards to first identifying genes and promoters that are specific to the tumor microenvironment in order to then apply concepts of synthetic biology for early detection. Most importantly, the tumor microenvironment is often described as a case of chronic inflammation (Yang and Zhang, 2017). It is well known that areas demonstrating wound healing or inflammation are particularly prone to tumor formation, as in the frequently documented case of inflammatory bowel disease progressing to colon cancer, for example. On a molecular level, even the growth factors and immune cells involved in inflammatory and tumor microenvironments are similar. For example, fibrin deposition caused by vascular endothelial growth factor (VEGF) release is a key initial stage in wound healing as well as solid cancer formation (Dvorak, 2015). Furthermore, both inflammatory environments and tumor microenvironments are characterized by a high density of leukocytes (Yang

and Zhang, 2017). Clearly, isolating the tumor microenvironment through genetic targeting and application of synthetic biology proves to be a challenging task when keeping in mind the need for specificity and sensitivity in early cancer detection.

### ***Boolean Logic Gates***

Luckily, the synthetic biology-based technique of incorporating Boolean logic gates into biological sensors can help to refine diagnostic tools by manipulating cell signaling pathways (Wang and Buck, 2012). For example, the incorporation of a Boolean “AND” gate in an engineered synthetic cell circuit can ensure that a reporter is only produced when two inputs are present, as shown in **Figure 2** (Wang and Buck, 2012). The incorporation of a “NOT” gate can repress reporter release in the presence of other defined inputs (Wang and Buck, 2012). Boolean logic has been applied to many biological models, including a circuit designed for the detection and treatment of psoriasis (Schukur, Geering, Charpin-El Hamri, & Fussenegger, 2015). Thus, in regards to creating a biosensor that only detects the tumor microenvironment and not inflammatory environments, incorporation of Boolean logic gates in synthetic gene circuits could prove to be a successful route.

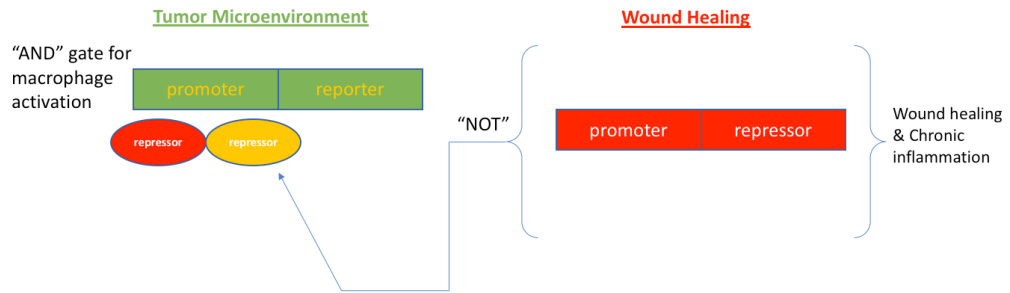


**Figure 2. Schematic depicting the use of Boolean logic gates to improve the specificity of an engineered cell circuit.** An “AND” logic gate helps define when a reporter signal should be produced, and a “NOT” logic gate outlines parameters where a reporter signal should not be produced (Wang and Buck, 2012).

### *Luciferase Reporters*

Secreted reporters pose as a useful method for monitoring activation of a promoter in cell culture media and *in vivo* because their expression can be quantified without cell lysis (Tannous, 2009). Reporter gene transcription corresponds with promoter activation, meaning that the level of secreted protein generally matches intracellular mRNA levels. Luciferase reporters code for oxidative enzymes that generate quantifiable bioluminescence (Tannous, 2009). *Gaussia* luciferase (Gluc) can also be detected intracellularly: approximately 5% of the reporter protein is not secreted, allowing for the use of bioluminescence imaging (Aalipour, 2019). This secreted reporter is from the marine organism *Gaussia princeps*, and can be detected in small microliter volumes of cell culture media, blood, and urine through the use of highly sensitive assays (Tannous, 2009).

## *Immunology and Cancer*

Cancer immunotherapy is a rapidly growing field of modern medicine. Traditional cancer therapy entailed use of surgery, radiation, and chemotherapy. Today, these techniques can now be used in combination with immunotherapies such as chimeric antigen receptor (CAR) T-cells, in order to reduce the amount of cytotoxic side effects caused by traditional cancer treatments. CAR T-cell therapy represents a form of adoptive cell transfer because a patient's own T-cells are isolated, genetically modified, and replaced in the patient (Miliotou & Papadopoulou, 2018). In the case of CAR T-cells, the immune cells are engineered to express receptors specific for antigens produced by the patient's tumor cells, allowing for a highly personalized and precise form of immunotherapy (Miliotou & Papadopoulou, 2018). One major drawback of CAR T-cell therapy is that it is primarily only effective in hematologic cancers, and is not yet efficacious in solid tumors (Klichinsky et al., 2017).

Recently, use of macrophages in cancer immunotherapy has become a novel area of interest. Macrophages are a natural waste-product during the isolation of a patient's T-cells during CAR T-cell therapy, and thus making use of them for alternate anticancer treatment modalities that can be used in conjunction with CAR-T cell therapy is promising (Moyes et al., 2017). Furthermore, macrophages exhibit excellent tumor-homing behaviors, and would be primarily effective in targeting solid cancers because of their ability to efficiently penetrate tumors and accumulate there (Alvey et al., 2017). Finally, as antigen presenting cells (APCs), macrophages will engulf tumor cells and present tumorigenic antigens, a process which activates T-cell response and helps induce

the body's natural immune response (Klichinsky et al., 2017). In fact, CAR macrophages (CARMA) have been developed as a way to engineer macrophages to phagocytose tumor cells (Klichinsky et al., 2017). Following the same principles of CAR T-cell therapy, CARMA are also engineered to express antigens specific to a patient's tumor (Klichinsky et al., 2017).

Genetically engineered macrophages (GEMs) are another avenue for use of macrophages in cancer immunotherapy (Moyes et al., 2017). The main purpose of GEMs is to alter the tumor microenvironment into an immunologically active state (Moyes et al., 2017). For example, macrophages are engineered to express proteins such as interleukin (IL) 21 that directly promote immune cell activation or indirectly prevent suppression of immune cell activity (Moyes et al., 2017). In this case, genetic engineering of macrophages is produced through the use of lentivirus transduction, a novel feat given the fact that macrophages naturally produce a restriction factor called SAMHD1, thereby traditionally preventing them from lentivirus transduction (Moyes et al., 2017). Inclusion of viral protein X in the lentivirus packaging allowed for the degradation of SAMHD1 and stable genetic delivery to human macrophages (Moyes et al., 2017).

Another approach to using macrophages for cancer immunotherapy comes through manipulation of SIRP $\alpha$ , a macrophage surface-protein that serves as a checkpoint for the CD47 marker, a "don't eat me" signal for macrophages (Alvey et al., 2017). Because tumor cells upregulate CD47, they are able to evade macrophage phagocytosis through the SIRP $\alpha$  pathway (Alvey et al., 2017). Upon injecting SIRP $\alpha$ -inhibited macrophages into mice, tumor regression was observed, suggesting how manipulation of

macrophage signaling pathways can pose as a potential pathway for new cancer treatments (Alvey et al., 2017).

While it is evident that immune cells and macrophages, specifically, have a growing role in cancer therapies, use of immune cells for cancer diagnostics is a less-explored field despite the cell type's natural tumor homing abilities.

### ***A Novel Field: Use of Immune Cells for Cancer Detection***

There is certainly a precedent for using living cell diagnostics for cancer detection (Danino et al., 2015). Many strains of bacteria demonstrate natural tumor homing abilities, primarily due to hypoxia and other features of the tumor metabolic environment, and are therefore convenient candidates for cancer detection (Danino et al., 2015). For example, using principles of synthetic biology, the *Escherichia coli* Nissle 1917 strain was engineered to produce a reporter detectable in urine upon homing to liver tumors (Danino et al., 2015). By using principles of synthetic biology, the use of living cell diagnostics can be expanded to include immune cells and specifically, macrophages, for early cancer detection with clinical translatability. Furthermore, administering immune cells such as macrophages has the added benefit that the immune cells will help destroy tumors when they detect an early cancer.

### ***Macrophage Biology***

Macrophages are part of the body's innate immune system, serving as phagocytotic cells and part of the body's first line of defense to pathogens and disease

(Parisi et al., 2018). While tissue-resident macrophages develop in utero and remain throughout one's life, recruited macrophages develop throughout life from hematopoietic stem cells and circulate as monocytes until they are recruited to specific tissues (Parisi et al., 2018). The proliferation and survival of recruited macrophages depends on activation of the colony stimulating factor 1 receptor (CSF-1R) on macrophages which binds both macrophage colony stimulating factor (M-CSF) and IL-34 (Garceau et al., 2010).

Once recruited to a specific microenvironment, macrophages further “activate” or mature to adopt a specific phenotype based on various metabolic and other biological stimuli in the environment due to their high level of plasticity (Martinez & Gordon, 2014). Traditionally, a dichotomy for macrophage polarization has been suggested: classically activated macrophages representing a “killer” or proinflammatory state are termed “M1s”, and alternatively activated macrophages represent a “builder” or anti-inflammatory state are termed “M2s” (Parisi et al., 2018). Each phenotype has a distinct metabolic profile and secretes unique cytokines to induct killer or builder pathways, as depicted in **Figure 3** (Parisi et al., 2018). Both phenotypes have roles in fighting against parasitic infections, and depending on the type of parasite and stage of disease, macrophages may polarize more towards one phenotype or another (Liu et al., 2014). For example, classically activated macrophages have microbicidal properties due to the upregulation of proinflammatory cytokines such as Interferon- $\gamma$  (IFN $\gamma$ ), as well as the increase in reactive oxygen species (ROS) and nitrogen radicals caused by the induction of genes such as inducible nitric oxide synthase (iNOS) (Liu et al., 2014). On the contrary, alternatively activated macrophages are key players in fighting helminth



infections, and also have regulatory and wound-healing roles due to the release of immunosuppressive cytokines such as IL-10 , which are important for wound resolution (Liu et al., 2014).

However, it has become apparent that the M1 and M2 dichotomy is too simple to encompass the different forms of activated macrophages. For example, tumor associated macrophages (TAMs) are macrophages containing different levels of both M1 and M2 properties depending on their spatial location in a tumor's metabolic environment (Carmona-Fontaine et al., 2017). The general scientific consensus is that TAMs are M2-like macrophages (Carmona-Fontaine et al., 2017). Tumors tend to recruit TAMs and M2s in order to generate an immunosuppressive environment that allows for tumor growth (Parisi et al., 2018).

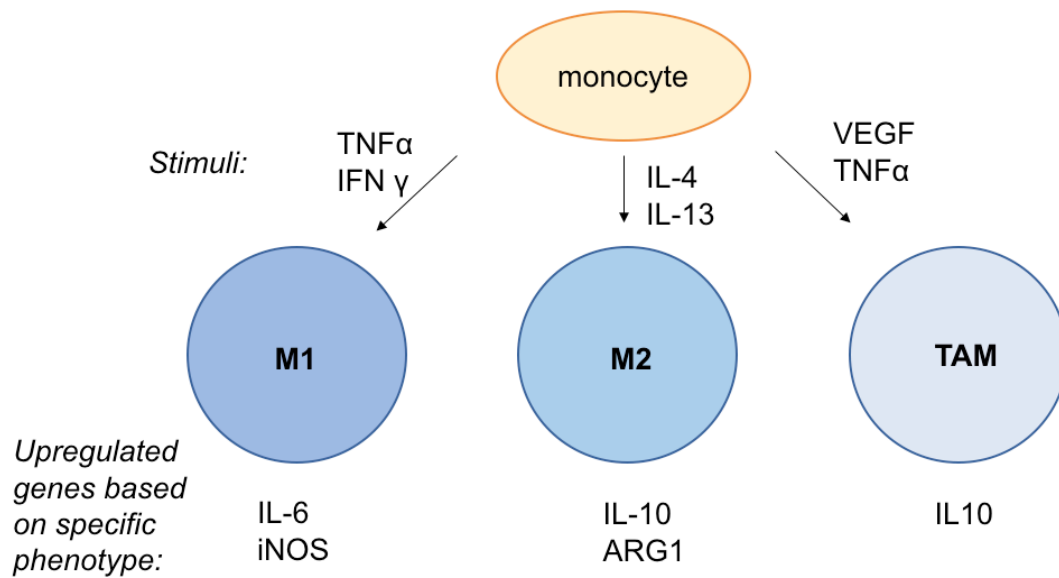


**Figure 3. A few macrophage polarization outcomes and their transcriptional profiles.** Note how stimuli and gene expression are not completely specific to a given macrophage phenotype. This figure does not represent a complete list of stimuli for macrophage polarization nor a complete list of genes upregulated in each phenotype. Figure adapted from (Parisi et al., 2018).

The different signaling pathways and features that drive macrophages to inflammatory and tumor microenvironments are important to consider in order to engineer macrophages using principles of synthetic biology as living cell diagnostics. While most cancer therapies utilize M1s to produce an anticancer effect, cancer detectors will mainly utilize M2s or TAMs because of their tumor homing nature.

### *Arginase 1*

Upregulation of Arginase 1 (ARG1) is a marker of M2 macrophages, and therefore of TAMs, which are M2-like (Liu et al., 2014). In the liver, ARG1 codes for a

key metabolic enzyme involved in the final stage of the urea cycle where it converts L-arginine to urea and L-ornithine (Pauleau et al., 2014). ARG1 is also upregulated in hematopoietic cells including M2 polarized macrophages where its function is less understood (Pauleau et al., 2014). Studies suggest that in M2s, the enzyme consumes the substrate arginine, thereby depleting its availability for nitric oxide synthases (Pauleau et al., 2014). Furthermore, secondary metabolites such as L-ornithine can be used for collagen biosynthesis (Pauleau et al., 2014).

The ARG1 promoter is ultimately activated by STAT6 activity (Pauleau et al., 2014). STAT6 is activated by cytokines such as IL4 and IL13, but it should be noted that IL4 and IL13 do not directly activate the ARG1 promoter (Pauleau et al., 2014). Three transcription factors are necessary for ARG1 promoter activation: PU.1, C/EBP, and STAT6 (Pauleau et al., 2014). The promoter does include an enhancer element that is IL4 responsive, but presence of the enhancer is not enough to trigger ARG1 expression (Pauleau et al., 2014). It should be noted that regions upstream of the transcriptional start site are constitutively active, indicating that the ARG1 promoter is “leaky” and will constantly be generating some amount of signal (Aalipour et al., 2019). Thus, fold changes in luminescence should be measured relative to baseline promoter activation in luciferase reporter assays.

### ***Proof of Concept Macrophage Sensor***

In a proof of concept study, macrophages have been used as immune cell sensors in mice to detect tumors as small as 4 mm<sup>3</sup>, thereby indicating that the macrophage

sensor is able to identify the early cancers that have potential to cause harm to the organism (Aalipour et al., 2019). In this model, macrophages are engineered to activate upon reaching a tumor metabolic environment, by activating the ARG1 promoter (Aalipour et al., 2019). Macrophages were transfected with a plasmid where activation of the ARG1 promoter is necessary for release of Gluc, the reporter signal. Because ARG1 gene expression is upregulated in M2s, the macrophage sensor is activated in the tumor microenvironment (Aalipour et al., 2019). Because Gluc is retained intracellularly in the macrophages and released into the blood, blood can be assayed to check for sensor activation through presence of Gluc, and subsequently, the tumor can be localized through bioluminescence imaging (Aalipour et al., 2019). See **Figure 4** for a general scheme of this proof of concept macrophage sensor.

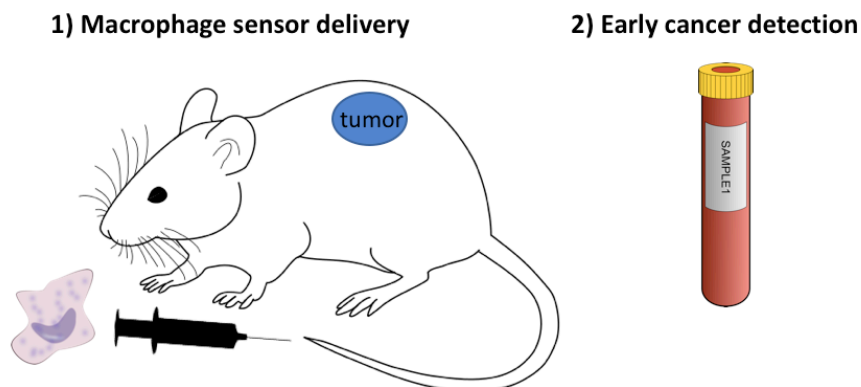


**Figure 4. Schematic for the use of macrophages as living cell diagnostics.** Engineered macrophages would be injected intravenously *in vivo* (1), and upon homing to tumors would activate and release a reporter signal that is detectable in blood (2).

### ***Improvements for the Macrophage Sensor***

Techniques of synthetic biology must be applied to make the macrophage sensor more specific for cancer detection. When applied *in vivo*, the macrophage sensor homes to confounding disease sites—mainly wound healing (Aalipour et al., 2019). In a mouse model of inflammation created with turpentine-oil in the hind leg, the macrophage sensor showed an increase in activation during the resolution phase of the wound healing process which generally begins on approximately day seven (Aalipour et al., 2019). The macrophage sensor did not show as much activation during the initial phase of wound healing, which is hallmarked by acute inflammation (Aalipour et al., 2019). During acute inflammation, macrophages are activated to be in an M1 state, whereas during resolution, the building phenotype, M2, is more prominent. Thus, it is understandable why there is false reporting by the macrophage sensor during the resolution phase of wound healing.

In order for this macrophage sensor to become an ideal tool for detecting and monitoring cancer, it must have sensitivity and specificity for small tumors. In other words, it must only produce a reporter signal in the presence of a tumor and not in other disease states.

### ***Specific Aims***

The goal of this thesis is to first polarize macrophages to the M1 and M2 phenotypes, in order to pave the way for analyzing genes upregulated in each phenotype. The purpose of genetic analysis is to identify genes that are solely upregulated in M1s

and not M2s and vice versa, with the hope of eventually incorporating these genes as “AND” and “NOT” gates in the macrophage sensor.

In this thesis, first, murine macrophage cells will be used to activate macrophages into the M1 and M2 phenotypes. In order to confirm that the polarization was successful, quantitative polymerase chain reaction (qPCR) or real-time reverse transcriptase PCR (RT-PCR) will be conducted to monitor for expression of ARG1 and iNOS genes, with ARG1 being a marker for M2 polarization and iNOS being a marker for M1 polarization. This polarization protocol will then be adapted for human monocyte cells as well, to ensure that the genes identified based on genetic analysis for logic gates will eventually be clinically translatable. To confirm that human macrophages have been polarized appropriately, regular PCR, ELISAs, and qPCR will be conducted to confirm gene expression of C-X-C motif chemokine 11 (CXCL11) and TNF $\alpha$  for the M1 phenotype, and gene expression of IL-10 for the M2 phenotype (Stossi, Madak-Erdogan, & Katzenellenbogen, 2012).

## METHODS

### *Macrophage Cell Lines*

To model murine macrophage cells, RAW264.7 cells were obtained from the American Type Culture Collection (ATCC). Cells were cultured in Dulbecco's Modified Eagle's Medium (DMEM) with 10% fetal bovine serum (FBS) and 1% antibacterial-antimycotic solution (ThermoFisher). Cells were maintained in a humidified 5% CO<sub>2</sub> incubator at 37 °C. Cells are mostly adherent cells, and therefore best scraped off the flask using a cell scraper between passages. Cells were maintained at a density between approximately  $3 \times 10^6$  and  $4 \times 10^6$  cells/mL. See **Figure 5** for typical RAW264.7 morphology.

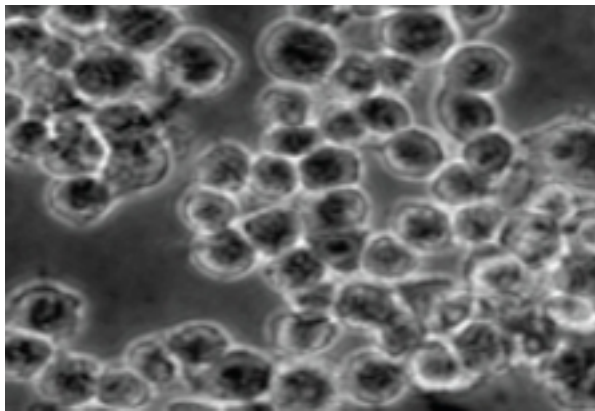


**Figure 5. RAW264.7 cells viewed with a 400x optical microscope.** These cells adopt a small and round morphology, but tend to grow in clusters. These cells grow well when maintained at a relatively high density. Figure taken from (Kang et al., 2010).

To model human monocyte cells, the THP-1 cell line was obtained from the ATCC. The culturing protocol was adapted from the Bowdish Lab, McMaster University, Ontario, Canada. Cells were cultured in RPMI supplemented with 10% FBS and 1%

antibacterial-antimycotic solution. Additionally, 2-mercaptoethanol (ThermoFisher) was added to media while passaging cells in order to reach a final concentration of 0.05 mM to help maintain a reducing environment (Bowdish, 2011). These suspension cells were maintained at a density between  $1 \times 10^5$  and  $1 \times 10^6$  cells/mL (Bowdish, 2011).

In order to activate macrophages into M1 and M2 polarized macrophages, cytokines must be added to the culture media. Because the RAW264.7 cells are murine macrophages, just 24 hours after plating the cells, cytokines can be added to the media in order to activate the macrophages to the M1 and M2 phenotypes. On day one,  $1 \times 10^6$  RAW264.7 cells are plated in 6-well plates in 2.5 mL media. After 24 hours of incubation, murine macrophage cells are activated to the M1 and M2 state by adding cytokines to the media or replacing the media with tumor conditioned media (TCM) in the 6-well plates. To generate M1s, IFN $\gamma$  was added to reach a final concentration of 100 ng/mL and to generate M2s, IL4 and IL13 were added in combination at a concentration of 25 ng/mL for each cytokine. IL4 and IL13 are key factors involved in immune suppression, whereas IFN $\gamma$  triggers immune cell responses to viral and bacterial infections (Martinez & Gordon, 2014). Macrophages were incubated in TCM to generate TAM phenotypes. TCM was collected from the murine carcinoma cell line, CT26 (ATCC). To prepare TCM,  $2.5 \times 10^5$  CT26 cells were plated in 6-well plates with 2.5 mL media per well. After 24 hours of incubation, the media was extracted and centrifuged for 10 minutes at 300 g. The supernatant was then used as TCM and was incubated with the macrophage cells. The 6-well plates were allowed to incubate for 24 hours with the cytokines or TCM for activation to occur. Thus, obtaining polarized murine macrophages



required a total of 48 hours, in order to first plate the macrophage cells and subsequently polarize them appropriately.

On the other hand, because the THP-1 cell line is a human monocyte cell line rather than a macrophage cell line, these cells must first be changed into macrophages before they can be further polarized. THP-1 cells were plated in T25cm<sup>2</sup> cell culture flasks (Corning) with  $1 \times 10^6$  cells in each flask, and 5 mL RPMI media. After 24 hours of incubation, the suspension monocyte cells were induced to become adherent macrophage cells by addition of phorbol myristate acetate (PMA) (Sigma-Aldrich) at a concentration of 100 ng/mL (Stossi, Madak-Erdogan, & Katzenellenbogen, 2012). After 24 hours of incubation with PMA, media was changed to fresh RPMI without PMA, and cells were allowed to incubate for six more days (Stossi, Madak-Erdogan, & Katzenellenbogen, 2012). During this six day incubation period, cells were washed and passaged three times, or in other words, media was changed every two days (Stossi, Madak-Erdogan, & Katzenellenbogen, 2012). After six days of incubation as adherent cells, the unpolarized activated macrophages, termed to be in the “M0” state, were ready for activation. To generate M1s, LPS was used alone at a concentration of 100 ng/mL or used in combination with IFN $\gamma$  (Stossi, Madak-Erdogan, & Katzenellenbogen, 2012). When added in combination, LPS was added to reach a final concentration of 100 ng/mL and IFN $\gamma$  to reach a final concentration of 20 ng/mL (Stossi, Madak-Erdogan, & Katzenellenbogen, 2012). LPS and IFN $\gamma$  were allowed to incubate with the cells for 4 hours only (Stossi, Madak-Erdogan, & Katzenellenbogen, 2012). LPS binds to the CD14 receptor on macrophages and triggers the release of cytokines and subsequent immune

inflammatory response (Sharp, 2013). To generate M2s, IL4 and IL13 were added in combination for a 24 hour incubation period, and were both used at a final concentration of 100 ng/mL (Stossi, Madak-Erdogan, & Katzenellenbogen, 2012). See **Figure 6** for typical morphology of THP-1 cells under different treatment conditions. For incubating with the human macrophage cells, TCM was collected from the human cervical cancer cell line, HeLa (ATCC), and was prepared by plating  $5 \times 10^6$  HeLa cells the day before it was used as TCM for macrophage activation. TCM was prepared following the same method as for murine macrophage activation.

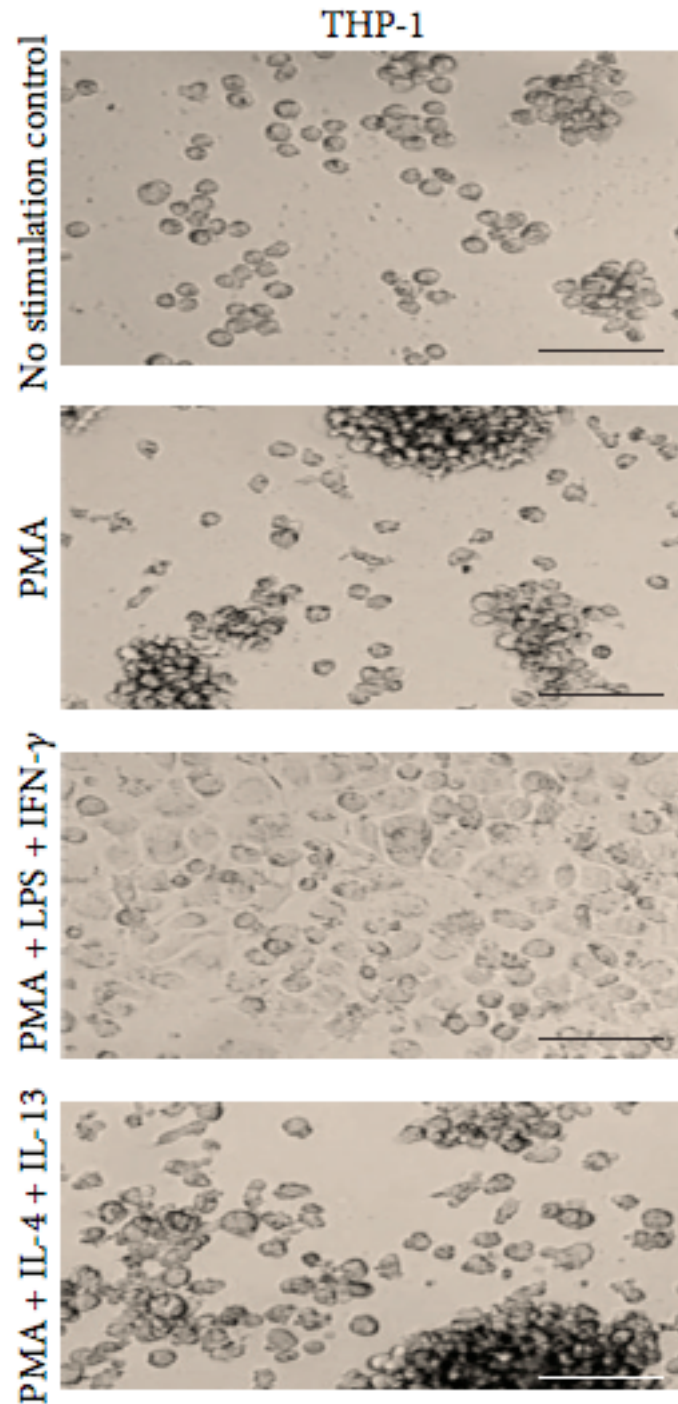


**Figure 6. THP-1 cells viewed with a 200x optical microscope under different treatment conditions.** Addition of PMA causes the macrophages to become adherent and responsive to cytokine activation. The scale bar represents 50  $\mu\text{m}$ . Figure taken from (Chimal-Ramirez, Espinoza-Sanchez, Chavez-Sanchez, Arriaga-Pizano, and Fuentes-Panana, 2016).

For both cell lines, M0 macrophages were also created by following the same protocols for murine and human polarized macrophages but without the addition of any cytokines or TCM to their incubation media.

### ***RNA Expression Analysis***

The 6-well plates were centrifuged for 5 minutes at 300 x g, and media supernatant was removed from all wells. Qiazol lysis reagent was added to the cell pellets and saved in Eppendorf tubes (Qiagen). RNA extraction was conducted using the Direct-zol RNA Miniprep Kit and protocol (Zymo Research).

RNA yield was assessed using the NanoDrop One Microvolume UV Spectrophotometer (ThermoFisher). 1000 ng of extracted RNA was used to make cDNA, using the iScript cDNA synthesis kit and protocol in 20  $\mu$ L reactions (Bio-Rad). All thermal cycling was conducted using the CFX96 Real-Time System C1000 Touch Thermal Cycler (Bio-Rad). For cDNA synthesis, the following protocol was used: 25°C for 5 min, followed by 46°C for 20 min, and finally, 95°C for 1 min.

The 2x SsoAdvanced Universal Probes Supermix (Bio-Rad) was used to conduct qPCR reactions for assessing iNOS, ARG1, and GAPDH expression in activated murine macrophages, and IL-10 expression in activated human macrophages. The volume of each qPCR reaction was 20  $\mu$ L, consisting of 2  $\mu$ L of cDNA synthesized from the iScript cDNA synthesis reactions, 10  $\mu$ L of SsoAdvanced Universal Probes Supermix, 1  $\mu$ L of FAM fluorophore-conjugated hydrolysis probes for either ARG1, iNOS, or

glyceraldehyde 3-phosphate dehydrogenase (GAPDH), and 7  $\mu$ L of nuclease-free water. All reactions were plated in duplicate on a clear-bottom 96-well plate (Bio-Rad). All products, including the gene-specific hydrolysis probes were obtained from Bio-Rad. Negative control reactions were conducted by replacing the 2  $\mu$ L of cDNA with 2  $\mu$ L of nuclease-free water. Thermal cycling was conducted at 95°C for 3 min, followed by 60 cycles of 95°C for 15 seconds and 59°C for 30 seconds. CFX Manager Software Version 3.1 was used to automatically generate a single cycle threshold and subsequent quantitation cycle ( $C_q$ ) values. Baseline subtraction was conducted for target gene expression relative to GAPDH. The Pfaffl method was used for relative quantification of gene expression for the different macrophage activation treatment conditions (Pfaffl, 2001).

The 2x ddPCR Supermix for Probes (Bio-rad) was used to conduct PCR reactions to assess CXCL11 expression in activated human macrophages. The volume of each PCR reaction was 25  $\mu$ L, consisting of 2  $\mu$ L of cDNA, 12.5  $\mu$ L of 2x ddPCR Supermix for Probes, 1  $\mu$ L each of forward and reverse primers for CXCL11, and 8.5  $\mu$ L of nuclease-free water. Thermal cycling was conducted at 95°C for 10 min, followed by 40 cycles of 94°C for 30 seconds and 60°C for 1 min, and ending with 98°C for 10 min. Gels were composed of 1% UltraPure Agarose (Invitrogen) in UltraPure Tris/Borate/EDTA (TBE) Buffer (Invitrogen), with addition of SYBR Safe DNA Gel Stain (ThermoFisher). 10  $\mu$ L of each PCR sample was loaded, and allowed to run for 30 min at 80 V. Gels were visualized under ultraviolet (UV) light in the UV Transilluminator BioDoc-It System Model M-26 (Avantor).

### ***ELISA Cytokine Analysis***

To assess TNF $\alpha$  and IL10 expression in activated human macrophages to confirm M1 and M2 polarization respectively, ELISAs were conducted using the Human TNF $\alpha$  ELISA MAX Standard Set and Human IL-10 ELISA MAX Standard Set and associated protocols (BioLegend). Assay diluent (BioLegend) was used as the zero standard. The 250 pg/mL top standards were diluted with six two-fold serial dilutions in order to generate standard curves for each cytokine. Computer-based curve-fitting software was used to generate the standard curve with concentration on the x-axis and absorbance on the y-axis.

All samples were plated in triplicate. The final absorbance of each sample was calculated as the absorbance at 570 nm subtracted from the absorbance at 450 nm. The concentration of TNF $\alpha$  and IL-10 in each sample was calculated based on the standard curve equations generated for each standard.

### ***Identifying Gene Candidates for “AND” and “NOT” Gates***

In order to identify genes that are M1-specific and M2-specific, the Immune Oriented Prediction of Clinical Outcomes from Genomics (iPRECOG) Signature Matrix was used (Stanford University, 2019). This database quantifies gene expression from 22 different immune cell phenotypes, including M1 and M2 macrophages, with gene expression validated using the CIBERSOFT method (Newman et al., 2015). The database was analyzed to select candidate genes for “AND” and “NOT” gates. Expression of

candidate genes expressed in M1 and M2 human macrophages was assessed using qPCR following the aforementioned protocol.

## RESULTS

### *Murine Macrophage Polarization*

In order to confirm successful M1 and M2 polarization, qPCR was conducted to compare gene expression of iNOS and ARG1 in RAW264.7 cells treated with different conditions. Using the Pfaffl method for relative quantification of gene expression allows for a ratio comparison of the change in gene expression relative to a baseline for different treatment conditions. qPCR Results are shown in **Table 1 and 2**.

**Table 1. Relative ARG1 expression in RAW264.7 cells that have been activated to become polarized macrophages with different treatment conditions.**

	ARG1 expression
<b>IL-4 + IL-13 treatment (M2)</b>	<b>74.028</b>
IFN $\gamma$ treatment (M1)	0.396
TCM treatment (TAM)	1.079

**Table 2. Relative iNOS expression in RAW264.7 cells that have been activated to become polarized macrophages with different treatment conditions.**

	iNOS expression
IL-4 + IL-13 treatment (M2)	1.505
<b>IFN<math>\gamma</math> treatment (M1)</b>	<b>29.446</b>
TCM treatment (TAM)	0.350

### *Human Macrophage Polarization*

In order to confirm successful M1 and M2 polarization, three tests were conducted. Regular PCR was conducted to confirm gene expression of CXCL11 in THP-



1 cells treated with LPS and IFN $\gamma$ . An ELISA for TNF $\alpha$  was conducted to further confirm TNF $\alpha$  expression in THP-1 cells treated with LPS and IFN $\gamma$ , and an ELISA was also conducted for IL-10 to confirm its expression in cells treated with IL-4 and IL-13. qPCR was conducted to confirm elevated gene expression of IL-10 in THP-1 cells treated with IL-4 and IL-13. PCR Results are shown in **Figure 7**, ELISA results are shown in **Figure 8 and Figure 9**, and qPCR results are shown in **Table 3 and Figure 10**.

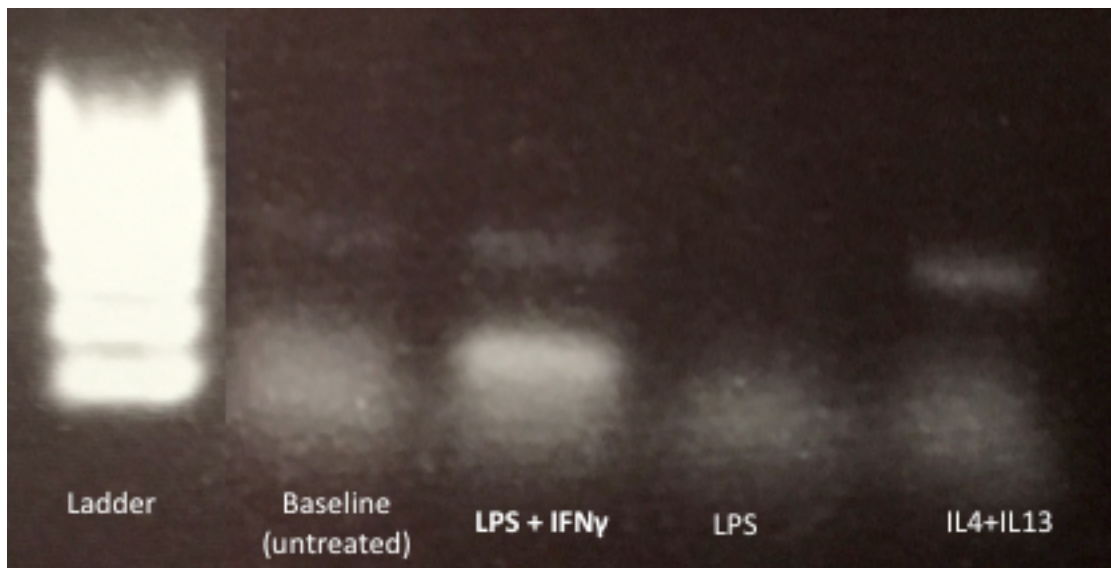


**Figure 7. CXCL11 expression is strongest in THP-1 cells treated with LPS and IFN $\gamma$ , or in M1 polarized macrophages.** CXCL11 is a marker for M1 macrophages and is not highly expressed in M2s (Stossi, Madak-Erdogan, & Katzenellenbogen, 2012).

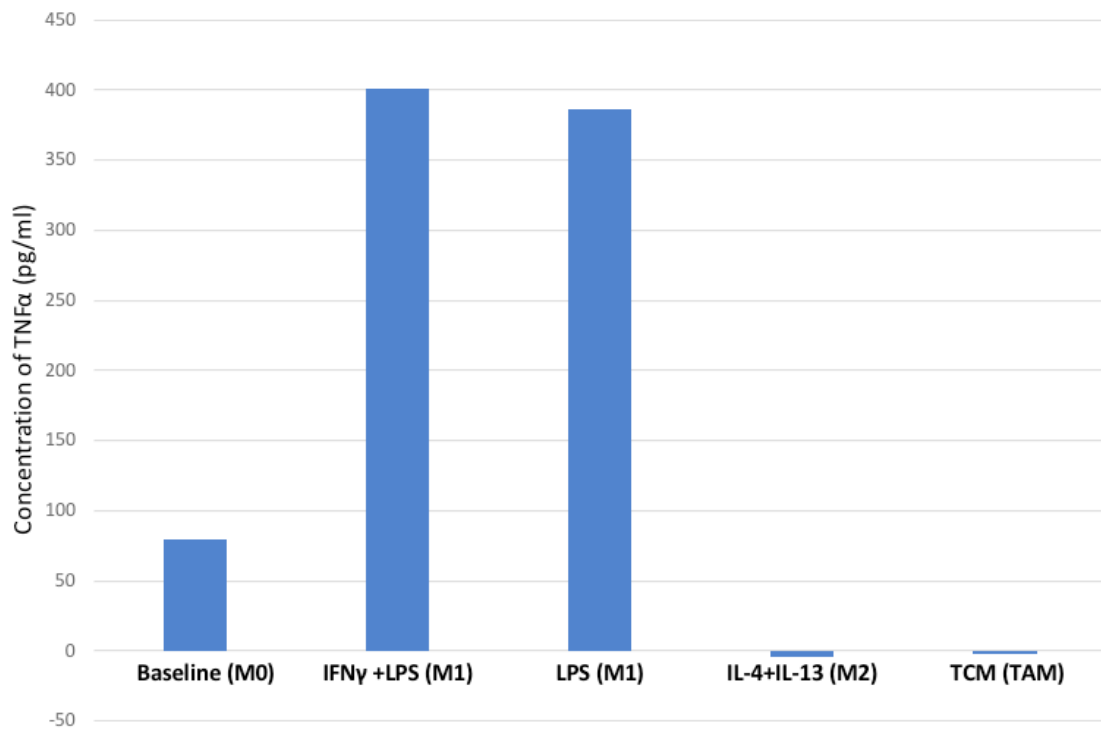


**Figure 8. ELISA result for TNF $\alpha$  expression in THP-1 cells that have been activated to become macrophages with different treatment conditions. TNF $\alpha$  expression is the highest in cells treated with IFN $\gamma$  and LPS, or M1 polarized macrophages. TNF $\alpha$  is an M1 marker.**

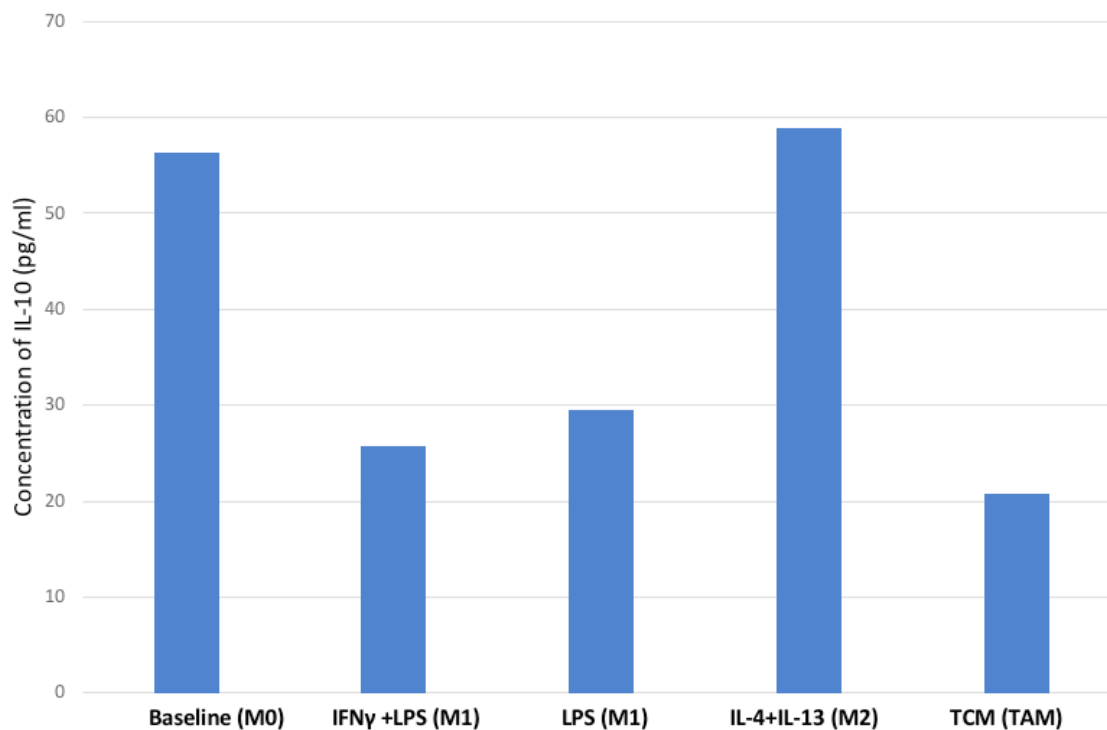


**Figure 9. ELISA result for IL-10 expression in THP-1 cells that have been activated to become macrophages with different treatment conditions. IL-10 expression is the highest in cells treated with IL-4 and IL-13. IL-10 is an M2 marker.**

**Table 3. Relative IL-10, an M2 marker, expression in THP-1 cells that have been activated to become polarized macrophages with different treatment conditions.**

	IL-10 expression
IL-4 + IL-13 treatment (M2)	8.545
LPS treatment (M1)	1.000

### *Identification of “AND” and “NOT” Gates*

Seven potential “NOT” gate candidates and four potential “AND” gates were found in the iPRECOG database. “AND” gate gene candidates are listed in **Table 4**, and “NOT” gate candidates are listed in **Table 5**.

**Table 4. Genes upregulated in M2s and expressed at low levels in M1s, identified using iPRECOG data (Stanford University, 2019).**

<b>Gene</b>	<b>M2</b>	<b>M1</b>	<b>Fold induction in M2</b>
CCL23	5505.22	615.57	8.94
HRH1	2195.07	145.28	15.11
CLEC10A	5770.13	69.4	83.14
DPEP2	2410.19	16.22	148.59

**Table 5. Genes upregulated in M1s and expressed at low levels in M2s, identified using iPRECOG data (Stanford University, 2019).**

<b>Gene</b>	<b>M1</b>	<b>M2</b>	<b>Fold induction in M1</b>
AQP9	4309.34	399.48	10.79
MSC	1562.14	101.48	15.39
APOBEC3A	4501.14	148.8	30.25
CYP271B	6662.56	145.7	45.73
SPIB	1435.06	31.21	45.98
CCL5	16862.2	250.75	67.25
CCL19	32553.9	137.07	237.50

### ***Testing Gene Candidates from the iPRECOG Database***

The genes for dipeptidase 2 (DPEP2), histamine receptor H1 (HRH1), and Spi-B transcription factor (SPIB) were randomly selected to test their expression levels in M1 and M2 human macrophages prepared from the THP-1 cell line, in order to reproduce the results displayed in the iPRECOG database. qPCR results are displayed in **Tables 6, 7, and 8.**

**Table 6. Relative DPEP2 expression levels in polarized macrophages prepared from the THP-1 cell line.<sup>1</sup>**

	<b>DPEP2 expression</b>
M1	3.936
M2	0.803

<sup>1</sup> Gene expression levels were obtained by conducting qPCR. According to the iPRECOG database, DPEP2 is upregulated in M2s (Stanford University, 2019).

**Table 7. Relative HRH1 expression levels in polarized macrophages prepared from the THP-1 cell line.<sup>1</sup>**

	<b>HRH1 expression</b>
M1	0.933
M2	3.259

<sup>1</sup> Gene expression levels were obtained by conducting qPCR. According to the iPRECOG database, HRH1 is upregulated in M2s (Stanford University, 2019).

**Table 8. Relative SPIB expression levels in polarized macrophages prepared from the THP-1 cell line.**

	<b>SPIB expression</b>
M1	0.158
M2	14.221

<sup>1</sup> Gene expression levels were obtained by conducting qPCR. According to the iPRECOG database, SPIB is upregulated in M1s (Stanford University, 2019).

## DISCUSSION

The goal of this research was to improve the specificity of the existing macrophage sensor, by identifying genes specific to the M1 and M2 phenotypes so that they could be implemented as Boolean logic gates. In summary, macrophage polarization into M1 and M2 phenotypes was accomplished for RAW264.7 and THP-1 cells. For both cell lines, M2 polarization was best achieved through combination IL-4 and IL-13 cytokine treatment. However, for the RAW264.7 cell line, M1 polarization was best accomplished with the use of IFN $\gamma$  alone, whereas for the THP-1 cell line, M1 polarization was best accomplished with combination treatment of IFN $\gamma$  and LPS. Finally, four potential “AND” and seven potential “NOT” gate targets were identified using the iPRECOG database (Stanford University, 2019). However, when expression of these genes was assessed in M1 and M2 macrophages activated from the THP-1 cell line, gene expression levels did not always correspond with gene expression levels provided in the iPRECOG database.

### ***RAW264.7 Cell Line***

The RAW264.7 macrophage cell line can be challenging to manage. Because of the fast growing nature of these macrophage cells featuring an 11 hour doubling time, the cells must be passaged frequently (Sakagami et al., 2009). However, the cells also grow best when plated at a subcultivation ratio between 1:3 and 1:5, and therefore should not be plated at an extremely low density despite their fast growth rate. Furthermore, the macrophage cells are healthiest when they are not too confluent, and therefore should be

maintained at a confluence density of around 70%. The cells will grow in clumps, particularly when cell culture flasks are becoming too confluent. Thus, it is important to constantly monitor the RAW264.7 macrophage cells and culture them at an appropriate density.

### ***Macrophage Polarization Methods for RAW264.7***

Many different activation methods for RAW264.7 were explored before concluding that combination IL-4 and IL-13 treatment was the best method for M2 activation, and IFN $\gamma$  treatment was the best method for M1 activation. For example, IL-4 and IL-13 were used alone at a concentration of 25 ng/mL each, TNF $\alpha$  was used at a concentration of 100 ng/mL, and LPS was used at a concentration of 200 ng/mL, all for a 24 hour incubation period (Aalipour et al., 2019). In one experiment where IL-4 and IL-13 were used separately at a concentration of 25 ng/mL, IL-13 did not induce a high level of ARG1 expression in the activated macrophages, as is shown in **Figure 10**.



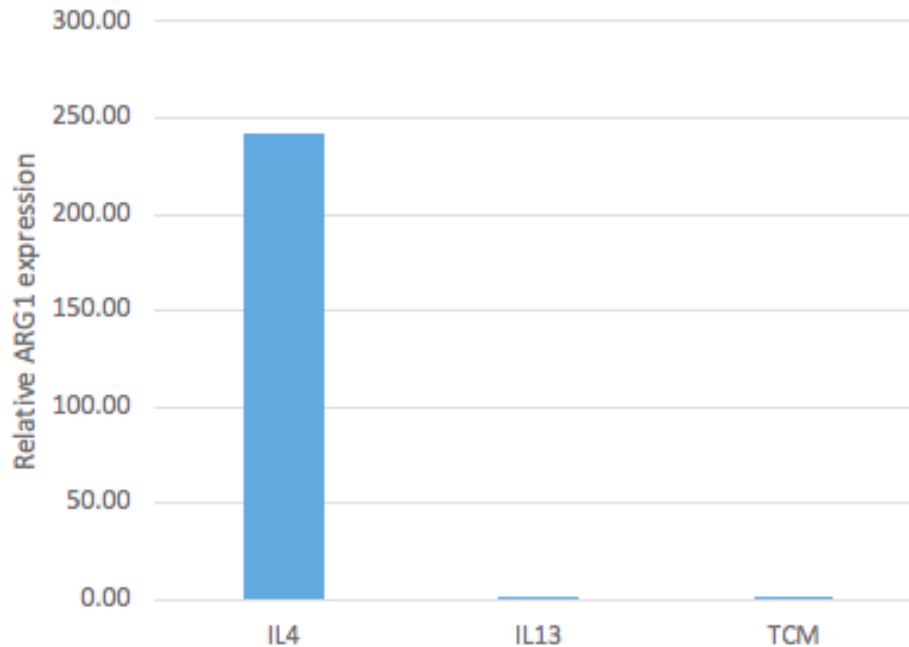


**Figure 10. Relative ARG1 expression in RAW264.7 cells treated with IL-4 alone and IL-13 alone compared to untreated cells.** IL-4 and IL-13 were both used at a concentration of 25 ng/mL. It is expected that IL-4 and IL-13 alone should each induce M2 polarization and therefore increased ARG1 expression.

One might wonder why IL-4 is simply not used without IL-13 to polarize murine macrophages into the M2 phenotype, given the greater than 200-fold upregulation of ARG1 observed for IL-4 treated cells in **Figure 10** compared to the approximately 70-fold upregulation of ARG1 observed for cells treated in combination in **Table 1**. First, it is important to note that fold-changes in gene expression can not simply be compared across qPCR data sets. This is because in each qPCR experiment, gene expression is normalized relative to GAPDH expression in that experiment. Though GAPDH expression is constant across all cells and is therefore a useful housekeeping gene used in all gene expression comparisons, in any given real-time RT-PCR experiment using

extracted RNA and subsequently synthesized cDNA, the numerical data values for GAPDH expression will vary slightly. Thus, GAPDH expression is accounted for every time in each qPCR experiment, such that results can be normalized for relative gene expression within each experiment. Therefore, one can only compare relative gene expression across experiments. For example, a conclusion that can be drawn by comparing results between experiments is that ARG1 expression was low in TCM-treated macrophages compared to IL-4 and IL-13 treated macrophages (see **Table 1** and **Figure 10**). However, one can not assume that IL-4 used alone induces more ARG1 expression than when used in combination treatment with IL-13 without further experimentation and data analysis.

Furthermore, it has been proven and is widely accepted in the scientific community that both IL-4 and IL-13 whether used alone or in combination are successful in polarizing macrophages to the M2 state (Sinha, Clements, Ostrand-Rosenberg, 2005). Thus, it is premature to conclude that IL-13 is ineffective in activating M2s, and further experimentation must be done in order to do so.

Furthermore, TNF $\alpha$  and LPS were used as treatments to induce the M1 phenotype. TNF $\alpha$  was unsuccessful in inducing iNOS expression, and in fact, produced similar iNOS expression levels as cells treated with the IL-4 and IL-13 combination. In one experiment, the fold induction for iNOS expression in cells treated with TNF $\alpha$  was 2.4, and 1.5 for cells treated with a combination IL-4 and IL-13. On the other hand, LPS seemed to induce markers of both the M1 and M2 phenotype.

LPS actually caused the largest induction in iNOS expression across all treatment types—even greater than IFN $\gamma$ . LPS caused a 2,3090.3 fold induction in iNOS expression, while in the same experiment, IFN $\gamma$  only caused a 29.4 fold induction. However, LPS also triggered a 9.25 fold induction in ARG1 expression in the same experiment, suggesting that the LPS-activated macrophages expressed features of both M1s and M2s. LPS is a proinflammatory endotoxin released by Gram-negative bacteria, and is commonly used in the scientific community to induce M1 polarization (Martinez & Gordon, 2014). Thus, further experiments need to be conducted in order to create a protocol for M1 polarization of RAW264.7 cells using LPS. For example, perhaps a shorter incubation time with LPS will induce only M1 features. An alternative explanation for an upregulation of M1 and M2 markers in LPS-activated macrophages lies in the idea that the M1 and M2 dichotomy does not actually exist, and that all macrophages have features of M1 and M2 cells to different extents (Martinez & Gordon, 2014).

It was hypothesized that TCM would induce ARG1 expression or an M2-like phenotype, however, this was not observed. Based on this study, TCM prepared in this manner does not seem to be an effective M2 polarization technique.

### ***Human Monocyte Cell Lines***

Human monocyte cell lines are challenging to manage. Initially, the U-937 cell line was cultured in addition to THP-1 cells (ATCC). Polarization was also attempted with U-937 cells (Sharp, 2013). However, the U-937 cell line proved to be exceedingly

difficult to polarize. The cells seemed to be sensitive to the addition of PMA and cytokines, which were causing cell death. Since the THP-1 cells were easier to work with in regards to polarization, they were chosen for the purpose of establishing polarization protocols.

### ***Macrophage Polarization Methods for THP-1***

While M2 polarization was simply accomplished with use of IL-4 and IL-13, M1 polarization was attempted in three different ways before concluding that 4-hour incubation with LPS and IFN $\gamma$  was most effective for M1 polarization. Initially, LPS was added to THP-1 cells for a 24-hour incubation period. However, this resulted in cell death by the end of the incubation period. Therefore, in subsequent attempts, THP-1 cells were incubated with LPS for just 4 hours, and it was noted that this shorter incubation period did not impact cell survival. Though PCR results as shown in **Figure 7** indicate that M1 polarization was best accomplished by combined treatment of LPS and IFN $\gamma$ , the ELISA result for TNF $\alpha$  as shown in **Figure 8** as well as scientific literature suggest that LPS alone is enough to induce M1 polarization (Stossi, Madak-Erdogan, & Katzenellenbogen, 2012). It should be noted that PCR was chosen to check for CXCL11 expression rather than qPCR for no particular reason other than the availability of materials. Furthermore, use of ELISAs is a commonly accepted method for verifying human macrophage polarization (Stossi, Madak-Erdogan, & Katzenellenbogen, 2012).

### ***“AND” and “NOT” Gate Gene Candidates from the iPRECOG Database***

qPCR data for expression levels of DPEP2 and SPIB in M1 and M2 polarized macrophages (see **Tables 6 and 8**) was unexpected, as it did not correspond with relative gene expression levels denoted in the iPRECOG database (see **Tables 4 and 5**).

According to iPRECOG, DPEP2 should have been upregulated in M2s, and therefore could have served as a potential “AND” gate for the macrophage sensor, and SPIB should have been upregulated in M1s, and therefore could have served as a potential “NOT” gate (Stanford University, 2019). Results obtained from qPCR indicate the opposite results, as seen in **Tables 6 and 8**. However, qPCR results for HRH1 expression levels as seen in **Table 7** are consistent with the iPRECOG database, which suggests that M2s have higher HRH1 expression levels, as shown in **Table 4**.

First, it is important to note that the iPRECOG data as shown in **Tables 4 and 5** only indicates relative gene expression in M1 and M2 macrophages. All of the genes listed in the database are expressed to some extent in both phenotypes. This explains why DPEP2 and SPIB were found to be expressed in both the M1 and M2 phenotypes in this experiment (see **Table 6 and 8**), but does not explain why the relative gene expression levels in M1 and M2 phenotypes did not match data found in the iPRECOG database. Furthermore, data shown in **Tables 6 and 8** may not correspond fully with the iPRECOG database because in this experiment, gene expression was assessed using cell lines rather than primary cells. The data displayed in the iPRECOG database is based on the analysis of primary cells (Newman et al., 2015). Overall, further experimentation with primary cells is necessary in order to reproduce the results displayed in the iPRECOG database.

Then, candidate genes may be implemented as “AND” or “NOT” gates to add specificity to the macrophage sensor.

### ***Limitations***

The biggest limitation in this study is the use of immortalized cell lines rather than primary cells. Cell lines are commonly used in research, primarily because of their cost-effectiveness and ease of use (Kaur and Dufour, 2012). Using cell lines provides useful preliminary data which can help paint a picture that is useful in deciding whether or not a proposed experiment is feasible. However, ultimately, cells behave differently *in vivo* and feature different characteristics overall. Primary cells are isolated from tissues, and retain many of the characteristics and functions which they exhibit *in vivo* (Kaur and Dufour, 2012). Furthermore, the iPRECOG database contains data obtained from studying primary cells (Newman et al., 2015). Therefore, in order to reproduce conclusions drawn about relative gene expression in M1s and M2s based on the iPRECOG database, it is most appropriate to conduct qPCR using RNA extracted from primary cells, rather than cell lines. Overall, data from this series of experiments lacks full credibility until further experiments are conducting replacing the use of RAW264.7 and THP-1 cell lines with bone marrow derived monocytes from mice, or macrophages derived from human blood (Aalipour et al., 2019).

Another limitation of this study is the premise that distinctly polarized M1 and M2 macrophages exist *in vivo* (Martinez & Gordon, 2014). While there are markers for M1 and M2 macrophages that are generally accepted in the scientific community, it is

much more likely that *in vivo*, macrophages exhibit different densities of these markers depending on their location and role in a given microenvironment (Carmona-Fontaine et al., 2017). For example, macrophages that are located in more hypoxic microenvironments are more likely to exhibit increased levels of ARG1, an M2 marker (Carmona-Fontaine et al., 2017). Thus, macrophages that are closest to a tumor might express the highest levels of ARG1, as compared to other “builder” macrophages that are also M2s, but exhibit lower levels of ARG1 simply because they are located in a different pocket of the tumor microenvironment (Carmona-Fontaine et al., 2017). Maneuvering this unclear spectrum of polarization is another reason to use primary cells for further studies, rather than cell lines, in order to produce more realistic results.

Finally, the macrophage sensor is currently designed for detection of tumors in mice and other species where macrophages exhibit ARG1 expression (Aalipour et al., 2019). Unlike in mice, ARG1 is not expressed in human macrophages, but rather, is expressed in human neutrophils (Murray and Wynn, 2011). This means that the current macrophage sensor is not actually clinically translatable to humans unless the ARG1 promoter is replaced with a promoter that is expressed in human macrophages. The ARG1 promoter could be replaced with the promoter for a gene identified through the iPRECOG database that is upregulated in M2s (see **Table 4**).

### ***Next Steps***

Isolation of primary monocytes from mouse and human blood is the most important next step for this project. Isolation of murine monocytes can be done by

utilizing bone marrow from mouse tibias and fibias (Aalipour et al., 2019). Isolation of human monocytes can be done from buffy coats or whole blood samples.

After isolating primary cells, the macrophage polarization protocols that have been designed in this thesis should be adapted and tested for polarization accuracy by confirming gene expression of iNOS and ARG1 in mouse macrophages, and CXCL11, TNF $\alpha$ , and IL-10 in human macrophages. If polarization is successful, then relative gene expression of “AND” and “NOT” gene candidates identified from the iPRECOG database (see **Tables 4 and 5**) should be assessed in M1 and M2 human macrophages.

### ***Clinical Translation***

Due to species to species differences, use of Gluc does pose questions of immunogenicity for humans and other organisms (Tannous, 2009). Secreted embryonic alkaline phosphatase (SEAP) is a commonly used secreted human reporter protein isolated from the human placenta that can be detected in small blood samples (Nilsson et al., 2002). Thus, for the purpose of clinical translatability, it would be beneficial to replace the Gluc reporter gene with SEAP in order to reduce the risk of immunogenicity when introducing the macrophage sensor to human populations.

The ARG1 promoter is an integral part of the current macrophage sensor, because its activation determines when a reporter is produced—in other words, the activation of the ARG1 promoter determines the overall specificity of the macrophage sensor. However, because the ARG1 promoter is only upregulated in mouse M2s, continued use



of the ARG1 promoter poses a long-term challenge in regards to the clinical translatability of the project.

Therefore, it would be beneficial to explore the use of other immune cells for the purpose of early cancer detection. For example, since ARG1 is produced in human neutrophils rather than macrophages, *in vitro* testing of a neutrophil sensor could yield promising results. Neutrophils could be transfected with the existing plasmid containing the ARG1 promoter driving Gluc reporter expression in order to create a neutrophil sensor (Aalipour et al., 2019).

Furthermore, myeloid-derived suppressor cells (MDSCs) stand out as a promising replacement for macrophages in this project because human MDSCs also express ARG1, and are less prominent players in inflammatory and wound healing environments (Vasquez-Dunddel et al., 2013). ARG1 in MDSCs is activated by a different promoter than in murine macrophages (Vasquez-Dunddel et al., 2013). In MDSCs, ARG1 is activated by the STAT3 promoter instead of the STAT6 promoter (Vasquez-Dunddel et al., 2013). Overall, the development of a living immune cell sensor for early cancer detection has huge implications for revolutionizing clinical diagnostics.

## REFERENCES

- Aalipour A., Chuang H., Murty S., D'Souza A.L., Park S., and Gunsagar S.G. et al. "Engineered immune cells as highly sensitive diagnostic probes of disease." *Nature Biotechnology* 2019, no. 41587 (2019): 1-15. <https://doi.org/10.1038/s41587-019-0064-8>.
- Alvey C.M., Spinler K.R., Irianto J., Smith L., Tewari M., and Discher D.E. "SIRPA-Inhibited, Marrow-Derived Macrophages Engorge, Accumulate, and Differentiate in Antibody-Targeted Regression of Solid Tumors." *Current Biology* 27, (2017): 2065–2077. <https://doi.org/10.1016/j.cub.2017.06.005>.
- Auslander D., Eggerschwiler B., Kemmer C., Geering B., Auslander S., and Fussenegger M. "A designer cell-based histamine-specific human allergy profiler." *Nature Communications* 5, no. 4408 (2014): 1-8. <https://doi.org/10.1038/ncomms5408>.
- Bowdish D. "Maintenance & Culture of THP-1 Cells." *Bowdish Lab, McMaster University* (2011). <http://www.bowdish.ca/lab/wp-content/uploads/2011/07/THP-1-propagation-culture.pdf>.
- Carmona-Fontaine C., Deforet M., Akkari L., Thompson C.B., Joyce J.A., and Xavier J.B. "Metabolic origins of spatial organization in the tumor microenvironment." *Proceedings of the National Academy of Sciences of the United States of America* 114, no. 11 (2017): 2934-2939. <https://doi.org/10.1073/pnas.1700600114>.
- Chimal-Ramirez G.K., Espinoza-Sanchez N.A., Chavez-Sanchez L., Arriaga-Pizano L., and Fuentes-Panana E.M. "Monocyte Differentiation towards Protumor Activity Does Not Correlate with M1 or M2 Phenotypes." *Journal of Immunology Research* 2016, no. 6031486 (2016): 1-16. <http://dx.doi.org/10.1155/2016/6031486>.
- Colegio O.R., Chu N.Q., Szabo A.L., Chu T., Rhebergen A.M., and V. Jairam. "Functional polarization of tumour-associated macrophages by tumour-derived lactic acid." *Nature* 513, no. 13490 (2014): 559-563. <https://doi.org/10.1038/nature13490>.
- Danino T., Prindle A., Kwong G.A., Skalak M., Li H., and Allen K. et al. "Programmable probiotics for detection of cancer in urine." *Science Translational Medicine* 7, no. 289 (2015): 289 (2015): <https://doi.org/10.1126/scitranslmed.aaa3519>.
- Din M.O., Danino T., Prindle A., Skalak M., Selimkhanov J., and Allen K. et al. "Synchronized cycles of bacterial lysis for *in vivo* delivery." *Nature* 536, no. 18930 (2016): 81-85. <https://doi.org/10.1038/nature18930>.

- Dvorak H.F. “Tumors: Wounds that do not heal—Redux.” *Cancer Immunology Research* 3, no. 1 (2015): 1-11. <https://doi.org/10.1158/2326-6066.CIR-14-0209>.
- Garceau V., Smith J., Paton I.R., Davey M., Fares M.A., and Sester D.P. et al. “Pivotal Advance: Avian colony-stimulating factor 1 (CSF-1), interleukin-34 (IL-34), and CSF-1 receptor genes and gene products.” *Journal of Leukocyte Biology* 87, no. 5 (2010): 753-764. <https://doi.org/10.1189/jlb.0909624>.
- Hori S.S., Lutz A.M., Paulmurugan R., and Gambhir S.S. “A Model-Based Personalized Cancer Screening Strategy for Detecting Early-Stage Tumors Using Blood-Borne Biomarkers.” *Cancer Research* 77, no. 10 (2017): 2570–84. <https://doi.org/10.1158/0008-5472.CAN-16-2904>.
- International Atomic Energy Agency. “Annex I. Recent developments in nuclear medicine for cancer management: from nuclear medicine to molecular imaging.” *Nuclear Technology*, (2010): 57.
- Kang S., Han D., Park K., Park H., Cho Y., and Lee H. et al. “Suppressive Effect on Lipopolysaccharide-Induced Proinflammatory Mediators by *Citrus aurantium L.* in Macrophage RAW 264.7 Cells via NF-KB Signal Pathway.” *Evidence-Based Complementary and Alternative Medicine* 2011, no. 248592 (2011): 1-12. <http://dx.doi.org/10.1155/2011/248592>.
- Kaur G., and Dufour J.M. “Cell lines: Valuable tools or useless artifacts.” *Spermatogenesis* 2, no. 1 (2012): 1-5. <https://doi.org/10.4161/spmg.19885>.
- Klichinsky M., Ruella M., Shestova O., Kenderian S.S., Kim M.Y. and O’Connor R. et al. “Chimeric antigen receptor macrophages (CARMA) for adoptive cellular immunotherapy of solid tumors.” *Cancer Research* 77, no. 13 (2017): 4575. <https://doi.org/10.1158/1538-7445.AM2017-4575>.
- Liu Y., Zou X., Chai Y., and Yao Y. “Macrophage Polarization in Inflammatory Diseases.” *International Journal of Biological Sciences* 10, no. 5 (2014): 520-529. <https://doi.org/10.7150/ijbs.887>.
- Martinez F.O., and Gordon S. “The M1 and M2 paradigm of macrophage activation: time for reassessment.” *F1000Prime Reports* 6, no. 13 (2014): 1-13. <https://doi.org/doi:10.12703/P6-13>.
- Miliotou A.N., and Papadopoulou L.C. “CAR T-cell Therapy: A New Era in Cancer Immunotherapy.” *Current Pharmaceutical Biotechnology* 19, no. 1 (2018): 5-18. <https://doi.org/10.2174/1389201019666180418095526>.

- Moyes K.W., Lieberman N.A., Kreuser S.A., Chinn H., Winter C., and Deutsch G. “Genetically Engineered Macrophages: A Potential Platform for Cancer Immunotherapy.” *Human Gene Therapy* 28, no. 2 (2017): 200-215. <https://doi.org/10.1089/hum.2016.060>.
- Murray P.J., and Wynn T.A. “Obstacles and opportunities for understanding macrophage polarization.” *Journal of Leukocyte Biology* 89, no. 4 (2011): 557-563. <https://doi.org/10.1189/jlb.0710409>.
- Newman A.M., Liu C.L., Green M.R., Gentles A.J., Weiguo F., and Yue X. et al. “Robust enumeration of cell subsets from tissue expression profiles.” *Nature Methods* 12, no. 3337 (2015): 453-457. <https://doi.org/10.1038/nmeth.33>.
- Nilsson E.E., Westfall S.D., McDonald C., Lison T., Sadler-Riggelman I., and Skinner M.K. “An in vivo mouse reporter gene (human secreted alkaline phosphatase) model to monitor ovarian tumor growth and response to therapeutics.” *Cancer Chemotherapy and Pharmacology* 49, no. 2 (2002): 93-100. <https://doi.org/10.1007/s00280-001-0396-0>.
- Pauleau A.L., Rutschman R., Lang R., Pernis A., Watowich S.S., and Murray P.J. “Enhancer-mediated control of macrophage-specific arginase I expression.” *The Journal of Immunology* 172, no. 12 (2004): 7565-7573. <https://doi.org/10.4049/jimmunol.172.12.7565>.
- Parisi L., Gini E., Baci D., Tremolati M., Fanuli M., and Bassani B. et al. “Macrophage Polarization in Chronic Inflammatory Diseases: Killers or Builders?” *Journal of Immunology Research* 2018, no. 8917804 (2018): 1-25. <https://doi.org/10.1155/2018/8917804>.
- Pfaffl M.W. “A new mathematical model for relative quantification in real-time RT-PCR.” *Nucleic Acids Research* 29, no. 9 (2001): 2001-2007.
- Sakagami H., Kishino K., Amano O., Kanda Y., Kunii S., and Yokote Y. et al. “Cell Death Induced by Nutritional Starvation in Mouse Macrophage-like RAW264.7 Cells.” *AntiCancer Research* 29, no. 1 (2009): 343-347.
- Schukur L., Geering B., Charpin-El Hamri G., and Fussenegger M. “Implantable synthetic cytokine converter cells with AND-gate logic treat experimental psoriasis.” *Science Translational Medicine* 7, no. 318 (2015): 1-11. <https://doi.org/10.1126/scitranslmed.aac4964>.
- Shamsi M., and Islamian J.P. “Breast Cancer: Early Diagnosis and Effective Treatment by Drug Delivery Tracing.” *Nuclear Medicine Review* 20, no. 1 (2017): 45-48. <https://doi.org/10.5603/NMR.2017.0002>.

- Sharp B.M. “Conversation of the U937 Monocyte into ‘Macrophage-Like’ Populations Exhibiting M1 or M2 Characteristics.” *Wright State University Theses and Dissertations* (2013): 1-60.
- Sinha P., Clements V.K., and Ostrand-Rosenberg S. “Interleukin-13–regulated M2 Macrophages in Combination with Myeloid Suppressor Cells Block Immune Surveillance against Metastasis.” *Cancer Research* 65, no. 24 (2005): 11743-11751. <https://doi.org/10.1158/0008-5472.CAN-05-0045>.
- Stanford University. “iPRECOG Signature Matrix – LM22.” *PRECOG* (2019). [https://precog.stanford.edu/iPRECOG\\_sigmatrix.php](https://precog.stanford.edu/iPRECOG_sigmatrix.php).
- Stossi F., Madak-Erdogan Z., and Katzenellenbogen B.S. “Macrophage-Elicited Loss of Estrogen Receptor Alpha in Breast Cancer Cells via Involvement of MAPK and c-Jun at the ESR1 Genomic Locus.” *Oncogene* 31, no. 14 (2012): 1825-1834. <https://doi.org/10.1038/onc.2011.370>.
- Tannous B. A. “*Gaussia* luciferase reporter assay for monitoring biological processes in culture and *in vivo*.” *Nature Protocols* 4, no. 28 (2009): 1-10. <https://doi.org/10.1038/nprot.2009.28>.
- Umansky V., Blattner C., Gebhardt C., and Utikal J. “The Role of Myeloid-Derived Suppressor Cells (MDSC) in Cancer Progression.” *Vaccines* 4, no. 4 (2016): 1-16. <https://doi.org/10.3390/vaccines4040036>.
- Vasquez-Dunddel D., Pan F., Zeng Q., Gorbounov M., Albesiano E., and Fu J. et al. “STAT3 regulates arginase-I in myeloid-derived suppressor cells from cancer patients.” *The Journal of Clinical Investigation* 123, no. 4 (2013): 1580-1589. <https://doi.org/10.1172/JCI60083>.
- Wang B., and Buck M. “Customizing cell signaling using engineered genetic logic circuits.” *Trends in Microbiology* 20, no. 8 (2012): 376-384. <http://dx.doi.org/10.1016/j.tim.2012.05.001>.
- Yang L., and Zhang Y. “Tumor-associated macrophages: from basic research to clinical application.” *Journal of Hematology & Oncology* 10, no. 58 (2019): 1-12. <https://doi.org/10.1186/s13045-017-0430-2>.

**VITA**

